



OPEN

Mechanical properties and Freeze-Thaw durability of concrete modified with microencapsulated phase change materials

Zhitao Zheng^{1,2}, Wenbing Shen^{1,2}✉, Sheng Li¹, Chuang Li¹, Pengjia Yin¹, Mingjun Guan¹ & Jizhang Ha¹

Microencapsulated phase change materials (mPCM) emerge as sustainable thermal energy regulation additives for enhancing concrete durability in cold climates. This investigation systematically evaluates the dose-dependent effects of mPCM incorporation (0–12% cement replacement) on mechanical-strength development and freeze-thaw resistance through comprehensive mechanical testing, 100-cycle accelerated freeze-thaw evaluations, and quantitative microstructural analysis. The experimental findings reveal a critical biphasic relationship: Optimal 6% mPCM addition significantly enhances mechanical performance with 8.90%, 19.23%, and 30.72% improvements in compressive strength, flexural strength, and splitting tensile strength versus control, while maintaining exceptional frost durability (1.6% mass loss and <15% strength degradation post-freeze-thaw). Microstructural analysis reveals that 6% mPCM optimizes the pore structure of concrete by reducing pore size and moderately increasing porosity, thereby enhancing freeze-thaw durability. Beyond the critical 9% threshold, the concrete matrix becomes loose, leading to a decline in overall strength. The established dosage-property correlation provides practical guidance for cold-region concrete design, demonstrating that 6% mPCM incorporation achieves synergistic enhancement of load-bearing capacity and phase-change-enabled thermal stress mitigation.

Keywords Microencapsulated phase change material (mPCM), Concrete, Freeze-thaw resistance, Mechanical properties, Microstructure, Low-carbon material

With the global transition of the construction industry towards sustainability, low-carbon and environmentally friendly building materials have become a research focus. Although concrete exhibits excellent mechanical properties, its freeze-thaw resistance and durability often perform poorly under extreme climatic conditions, such as freeze-thaw cycles and temperature fluctuations^{1–3}. In regions with alternating hot and cold climates, freeze-thaw cycles lead to the expansion of micropores in concrete, forming microcracks that eventually develop into macrocracks. The expansion of freezing water and ice crystal growth exacerbate crack propagation, resulting in the degradation of mechanical properties, loss of durability, and even potential structural failure^{4,5}. These challenges limit the application of concrete in cold regions^{6,7}. Therefore, enhancing the freeze-thaw resistance and durability of concrete has become a crucial research direction in building materials.

In recent years, various modification approaches have been proposed to address freeze-thaw damage, including the addition of antifreeze agents, high-performance cement, waterproof coatings, and fiber-reinforced materials ^{8–10}. However, these methods often increase costs or compromise performance. For instance, traditional antifreeze agents tend to reduce concrete strength, while waterproof coatings, despite enhancing freeze-thaw resistance, have limited service life and require regular maintenance. In contrast, microencapsulated phase change materials (mPCM), as an emerging building material, effectively mitigate freeze-thaw damage due to their superior heat absorption and release properties, significantly improving both freeze-thaw resistance and durability. Additionally, mPCM improves the microstructure of concrete by reducing the formation of large pores, thereby enhancing not only its freeze-thaw performance but also its impermeability and crack resistance, demonstrating broad application prospects. By encapsulating phase change materials (PCM) within microcapsules, mPCM absorbs or releases heat during temperature fluctuations, improving the thermal performance and freeze-thaw resistance

¹2nd Construction Co.,LTD Of China Construction 5th Engineering Bureau, Hefei Anhui 230041, China. ²China Construction Fifth Engineering Bureau Co., Ltd, Changsha Hunnan 410000, China. ✉email: shenwbyh@163.com

of concrete while enhancing its thermal storage capacity, thereby mitigating the negative effects of freeze-thaw cycles^{11–14}. With advancements in PCM technology, increasing research efforts have integrated these materials into concrete to enhance building thermal comfort and energy efficiency¹⁵.

PCMs are generally classified into three types: organic, inorganic, and composite materials. However, their application in concrete still faces challenges related to stability and long-term performance, particularly due to expansion or contraction caused by temperature variations, which may affect the overall structural integrity of concrete. To address these issues, mPCM, as a novel composite material, effectively resolves the stability concerns of traditional PCM in concrete applications. By encapsulating PCM within microcapsules, mPCM not only enhances thermal stability but also precisely regulates heat absorption and release within specific temperature ranges, thereby improving the freeze-thaw resistance and thermal regulation of concrete. This characteristic makes mPCM an ideal temperature-regulating material, particularly suitable for environments with significant temperature fluctuations¹⁶. Furthermore, as a low-carbon and environmentally friendly material, mPCM reduces building energy consumption and greenhouse gas emissions¹⁷ highlighting its potential for green building applications.

Previous studies have demonstrated that incorporating mPCM improves the thermal performance of concrete while maintaining relatively stable compressive strength. Alsaadawi et al.¹⁸ investigated the effects of different mPCM dosages (1%, 3%, 5%, 7%, 10%) on the thermal performance of concrete and found that at dosages below 7%, thermal conductivity and heat capacity were optimized. However, studies have shown that with increasing mPCM content, the number of microcapsules within the concrete matrix rises significantly, resulting in more frequent collisions and compression during the mixing process. These interactions increase the likelihood of shell rupture. In addition, at higher dosages, localized heat accumulation and simultaneous phase transition may further elevate the internal pressure of the microcapsules, thereby promoting rupture¹⁹. Such rupture not only diminishes the thermal regulation capability of the mPCM but may also release the core material, leading to interfacial deterioration and a subsequent decline in the overall mechanical performance of the concrete. Cao et al.²⁰ explored the energy efficiency of geopolymers concrete (GPC) walls containing mPCM, concluding that increasing wall thickness and mPCM dosage significantly enhanced building energy efficiency. Pilehvar et al.²¹ reported that while mPCM incorporation reduced the compressive strength of GPC, the material retained relatively high strength and exhibited favorable thermal performance.

The influence of mPCM on the microstructure of concrete has also attracted attention. Djamai et al.²² conducted a series of experiments, including thermophysical and microstructural analyses, and observed that incorporating different PCM dosages (5%, 10%, and 15%) altered the pore structure of cementitious materials, particularly contributing to the formation of large pores, which could impact concrete performance. Although PCM incorporation improves certain thermal properties, excessive dosage may hinder cement hydration, leading to a decline in mechanical properties.

Li et al.²³ examined the thermal performance of PCM in building walls, particularly its effects on thermal conductivity and specific heat capacity. Their study showed that with increasing PCM content, the specific heat capacity of concrete increased linearly, while thermal conductivity gradually decreased. Sukontasukkul et al.²⁴ investigated the effects of high PCM content (up to 7.8%) on the thermal performance of lightweight concrete, revealing that as PCM content increased, the energy storage density exhibited a linear increase, while thermal conductivity decreased. The study also highlighted that the state of PCM (liquid or solid) and testing temperature significantly influenced thermal performance. Although PCM incorporation improved thermal performance and energy storage capacity, excessive amounts affected the pore structure and mechanical properties of concrete.

Although previous studies have explored the incorporation of mPCM in concrete, most have focused on its macroscopic mechanical properties, particularly in applications related to pavement de-icing and snow melting^{25–27}. However, the specific role of mPCM under freeze-thaw (F-T) conditions remains inadequately understood, especially regarding the correlation between pore structure evolution and frost resistance^{28,29} with limited experimental validation available. Therefore, further investigation using microstructural observations and physical performance analysis is essential to elucidate the mechanisms by which mPCM influences F-T durability in concrete. Such research would provide a stronger foundation for its practical application and facilitate more rational dosage optimization.

This study aims to experimentally analyze the performance of concrete incorporating microencapsulated phase change material (mPCM), with a particular focus on its freeze-thaw resistance. Specifically, different mPCM dosages (0%, 3%, 6%, 9%, and 12%) were evaluated for their effects on the compressive strength, flexural strength, and splitting tensile strength of concrete, alongside freeze-thaw cycle tests to assess the contribution of mPCM to concrete durability. Additionally, microstructural analysis was conducted to elucidate the underlying mechanisms by which mPCM improves freeze-thaw resistance, particularly through pore structure optimization and thermal regulation, which effectively suppress freeze-thaw-induced expansion damage and enhance durability. Furthermore, the application of mPCM in concrete has the potential to significantly reduce energy consumption and greenhouse gas emissions during the service life of buildings. As an environmentally friendly material³⁰ mPCM not only enhances the freeze-thaw resistance and durability of concrete but also aligns with the principles of green building design, offering innovative solutions for the sustainable development of the construction industry.

Experimental program

Materials

In this study, microencapsulated phase change material (mPCM) was prepared using microencapsulation technology, where phase change materials (PCMs) were encapsulated within protective shells to enhance their uniform distribution and long-term stability in concrete. PCM refers to a class of functional materials that absorb or release a large amount of latent heat through solid-liquid phase transitions in response to temperature

Material type	Shell	Core material	Appearance	Phase transition temperature	Enthalpy value	Solid content	PH value
Phase change nanomaterials	Modified polyurethane	C12-16 normal alkane	Milky liquid	6.5±1.5°C	161 J/g	40±1%	6.5-7.7

Table 1. Main physical and chemical properties of MPCM.

Group number	Water (kg · m ⁻³)	Cement (kg · m ⁻³)	River sand (kg · m ⁻³)	Gravel (kg · m ⁻³)	mPCM (kg · m ⁻³)	Water reducing agent (kg · m ⁻³)	Defoamer kg · m ⁻³)
P0	196	570	622	1012	0	4.56	0.46
P3	196	570	602	1012	25.6	4.56	0.46
P6	196	570	585	1012	37.5	4.56	0.46
P9	196	570	566	1012	56.0	4.56	0.46
P12	196	570	547	1012	75.0	4.56	0.46

Table 2. Raw material mix of concrete.

changes, making them widely used for thermal energy storage and regulation. Typical PCMs can be classified into organic types (e.g., paraffin and fatty acids), inorganic types (e.g., salt hydrates), and composite types (e.g., organic-inorganic hybrids). The fundamental property of PCM is its ability to undergo phase transition within a specific temperature range, efficiently storing and releasing energy through heat absorption and emission.

In low-temperature environments, PCM can effectively absorb the latent heat released during the freezing of water within concrete pores, thereby mitigating the frost heaving pressure caused by ice crystal expansion and reducing structural damage due to freeze-thaw cycles. Additionally, by slowing down the heat release rate, PCM helps suppress the formation of internal cracks induced by severe temperature fluctuations during freeze-thaw cycling, thereby enhancing the frost resistance and durability of concrete.

The key physicochemical properties of the multi-scale mPCM used in this study are summarized in Table 1. The mPCM consists of a modified polyurethane shell and a C12-16 n-alkane core, forming a microcapsule structure with phase change energy storage functionality. At room temperature, mPCM appears as a milky white liquid with high thermal storage and release capacity. Specifically, the phase transition temperature of mPCM is 6.5±1.5°C, at which its core material transitions from solid to liquid, absorbing environmental heat. Conversely, as the temperature drops, the liquid core material solidifies, releasing the stored thermal energy. Unlike water, which expands by approximately 9% during phase transition at 0 °C, mPCM exhibits minimal volumetric change during solid-liquid transformation, preventing additional expansion pressure and alleviating internal stress concentration in concrete during freeze-thaw cycles.

Moreover, the high phase change enthalpy of mPCM (161 J/g) allows it to absorb latent heat during early freezing, delaying ice nucleation and reducing frost-heaving pressure³¹. Although water eventually freezes, mPCM acts as a thermal buffer that smooths the freezing process, alleviates stress peaks, and helps delay microcrack formation during repeated F-T cycles³². This mechanism contributes to improved durability, as evidenced by reduced mass loss and better pore structure in mPCM-modified concrete.

Specimen Preparation

The concrete mix proportions used in this study are listed in Table 2. The specimens were categorized into plain concrete (P0) and microencapsulated phase change material (mPCM)-modified concrete (P3, P6, P9, P12), where P0, P3, P6, P9, and P12 correspond to mPCM dosages of 0%, 3%, 6%, 9%, and 12%, respectively. During specimen preparation, cement, fine aggregates, and coarse aggregates were first dry-mixed according to the designed proportions in a mixer for 90 s to ensure uniform distribution. Subsequently mPCM, superplasticizer, and defoamer were added into water in a predetermined ratio. A polycarboxylate-based superplasticizer was used to enhance the fluidity and water-reducing effect of the concrete, while a silicone-based defoamer was employed to minimize foam generation in the mixture. To ensure homogeneous dispersion of mPCM within the concrete matrix, an ultrasonic processor (Model: UP400S, Hielscher Ultrasonics, Germany) was applied with a power setting of 600 W for 1 h.

The prepared mPCM solution was then mixed with the dry materials using the encapsulated sand-coating method:

1. First Stage: Half of the mPCM solution was added and mixed for 60 s.
2. Second Stage: Cement was introduced, followed by an additional 60 s of mixing.
3. Final Stage: The remaining mPCM solution was incorporated, and mixing continued for another 120 s to ensure complete integration of cement and mPCM, resulting in a homogenous concrete mixture.

After mixing, the fresh concrete was poured into molds and compacted using a vibrator to remove air bubbles and enhance density. The specimens were initially cured in a controlled environment at a temperature of 20±2 °C and relative humidity≥95% for 24 h before demolding. Subsequently, they were subjected to standard curing conditions for 28 days to ensure the required strength and stability were achieved.

The specimen dimensions were as follows:

- 100 mm × 100 mm × 100 mm cubic specimens for compressive strength, splitting tensile strength, and freeze-thaw resistance tests.
- 100 mm × 100 mm × 400 mm beam specimens for flexural strength and freeze-thaw resistance tests.

Figure 1 illustrates the concrete mixing process.

Experimental methods

This study evaluates the effect of microencapsulated phase change material (mPCM) on the frost resistance of concrete, focusing on the mechanical properties and microstructural evolution during freeze-thaw (F-T) cycles. The experimental program includes F-T cycle tests, mechanical property assessments, and microstructural analyses to systematically investigate the modification mechanisms of mPCM.

The F-T cycle test was conducted following the *Standard for Test Methods of Long-Term Performance and Durability of Ordinary Concrete* (GB/T 50082 – 2009). A ZT-CTH-200 freeze-thaw testing chamber was used, where each cycle consisted of 8 h of freezing at -20 °C and 4 h of thawing at 18 °C. The specimens included 100 mm × 100 mm × 100 mm cubic samples and 100 mm × 100 mm × 400 mm prismatic beams. Five groups of tests were performed, with three specimens per group, evaluating mass loss, relative dynamic elastic modulus, and mechanical performance. During testing, specimen mass was measured after every 100 F-T cycles, and the dynamic elastic modulus was determined using a DT-W18 dynamic elastic modulus tester to assess the cumulative freeze-thaw damage.

The mechanical properties were tested in accordance with the *Standard for Test Methods of Physical and Mechanical Properties of Concrete* (GB/T 50081 – 2019), including compressive, flexural, and splitting tensile strength tests. Compressive strength was measured using a 3000 kN fully automatic compression testing machine (Instron, USA) at a loading rate of 0.5 MPa/s. Flexural strength was determined through a three-point bending test using an electro-hydraulic servo material testing machine (MTS Systems Corporation, USA). Splitting tensile strength was tested at a loading rate of 0.05 MPa/s until specimen failure. These tests were conducted before and after 100 F-T cycles to analyze the influence of mPCM on concrete's mechanical properties.

Microstructural analysis was performed using a NovaNanoSEM230 scanning electron microscope (SEM) (FEI, Netherlands) and a PoreMaster33 mercury intrusion porosimeter (MIP) (Quantachrome Instruments, USA). SEM was employed to observe the interfacial transition zone (ITZ) and pore characteristics of the concrete matrix before and after F-T cycles. The test samples, taken from the core regions of the specimens, were prepared into dimensions of 10 mm × 10 mm × 5 mm and coated with a gold layer before observation. MIP analysis was used to investigate pore structure evolution, with test samples also extracted from the specimen cores. Each test sample weighed approximately 5 g and was prepared as cylindrical specimens with a diameter of 10 mm and a height of 20 mm. Prior to testing, all samples were oven-dried at 105 °C for 24 h to remove free water, ensuring accurate results.

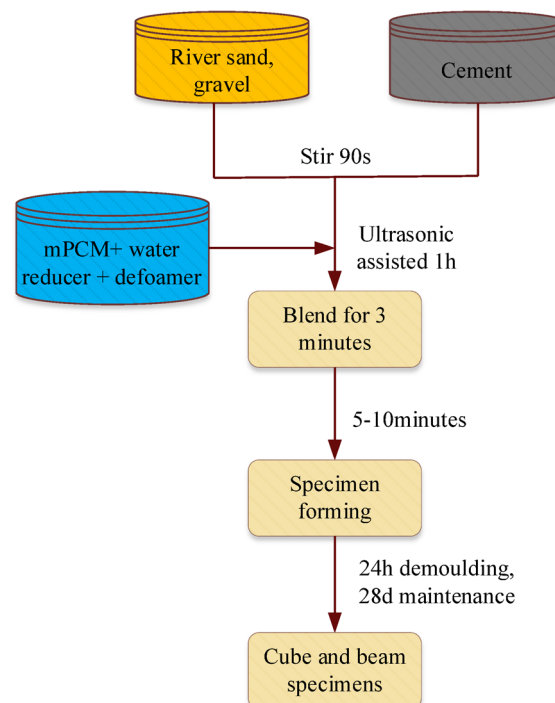


Fig. 1. mPCM concrete casting process.

Results and discussion

Effect of Freeze-Thaw cycles on the mechanical properties of concrete

Compressive strength variations

As shown in the experimental results in Fig. 2, the initial compressive strength of concrete decreases significantly with the incorporation of mPCM. The degree of reduction ranges from 7.1 to 24.8% as the mPCM dosage increases. This reduction is primarily attributed to the lower mechanical properties of mPCM itself, which, when replacing a portion of river sand, weakens the interlocking effect between aggregates, thereby reducing the compactness and overall load-bearing capacity of the concrete.

However, after 100 freeze-thaw (F-T) cycles, the compressive strength of P3 and P6 specimens increased by 2.7% and 8.9%, respectively, compared to the control group (P0). In contrast, the compressive strength of P9 and P12 specimens decreased by 9.7% and 19.5%, respectively, relative to P0. These results indicate that an appropriate mPCM dosage (e.g., 6%) can effectively enhance the frost resistance of concrete and maintain higher compressive strength throughout the F-T cycles.

The enhancement in compressive strength during F-T cycles is primarily due to the thermal regulation mechanism of mPCM. Specifically, mPCM absorbs heat during the freezing phase, reducing the internal temperature gradient of the concrete and mitigating the freezing expansion pressure exerted by pore water. This process limits the formation and propagation of microcracks. During the thawing phase, mPCM releases stored heat, accelerating the melting of ice crystals and thereby minimizing structural damage caused by ice crystal growth. As a result, the P6 specimens demonstrated superior compressive strength retention after 100 F-T cycles compared to other dosage levels. However, when the mPCM dosage increased beyond 9%, a decline of more than 13.9% in compressive strength was observed relative to P6. This suggests that excessive mPCM incorporation negatively impacts the frost resistance of concrete. High dosages may lead to a weakened interfacial transition zone (ITZ) between aggregates, compromising the compactness and structural integrity of the concrete.

Flexural strength variation

In this study, three specimens were prepared for each mix proportion. The reported values represent the average results, with error bars indicating the standard deviation to reflect data variability and reproducibility. As shown in Fig. 3, the data correspond to the flexural strength measured after freeze-thaw cycles. The flexural strength of concrete exhibits an initial increase followed by a decline with increasing mPCM content. Specifically, mPCM incorporation enhances the flexural strength of conventional concrete. The control group (P0) without mPCM exhibits a flexural strength of 5.20 MPa, while the P3 and P6 groups, containing 3% and 6% mPCM, respectively, achieve significant improvements, reaching 5.50 MPa and 6.17 MPa, corresponding to increases of 5.70% and 19.23%. However, when the mPCM content increases to 9% (P9), the flexural strength decreases by 11.35% compared to P6, and in the P12 group, it declines by 18.96%.

Thus, an appropriate amount of mPCM (such as 6%) significantly improves the flexural strength of concrete, likely due to the microstructural optimization provided by mPCM microcapsules. During freeze-thaw cycles, mPCM enhances the thermal regulation capacity of concrete, mitigating crack propagation and thus improving flexural strength. However, excessive mPCM content may weaken the bond strength of the cementitious matrix and hinder hydration reactions, leading to a decline in flexural strength. Therefore, the improvement in flexural strength is closely related to the suppression of microcracks and the mitigation of temperature gradients during freeze-thaw cycles, while excessive mPCM incorporation may have detrimental effects.

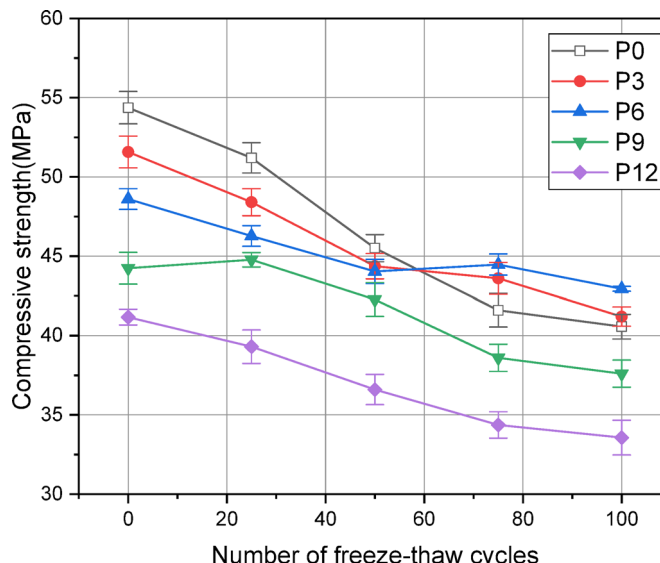


Fig. 2. Compressive Strength of mPCM-Modified Concrete.

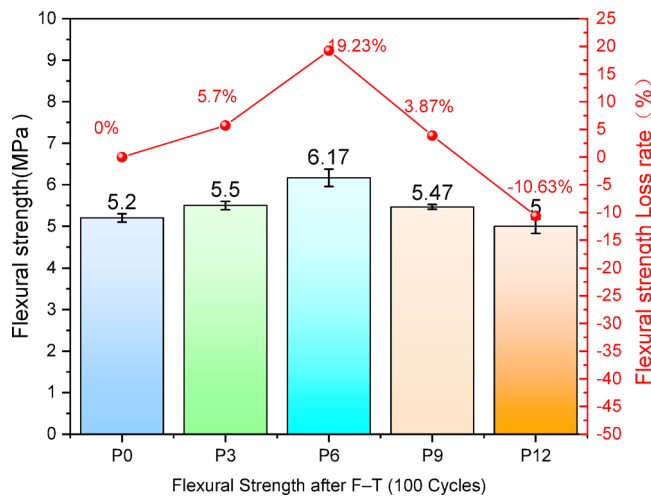


Fig. 3. Flexural Strength of mPCM-Modified Concrete.

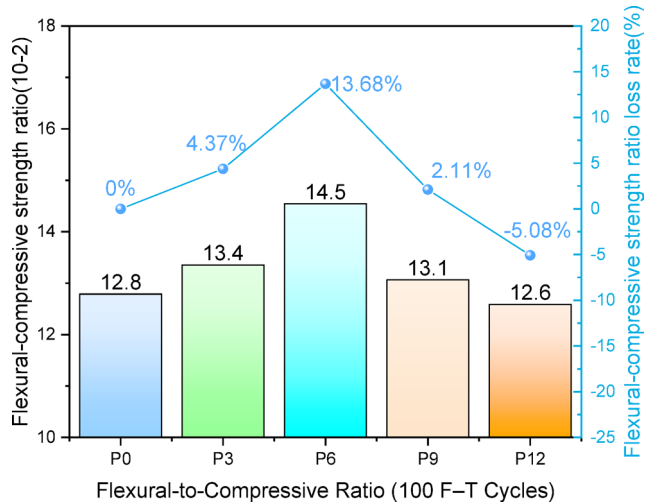


Fig. 4. Flexural-to-Compressive Strength Ratio of mPCM-Modified Concrete.

Flexural-to-Compressive strength ratio (FCR) variation

The toughness of concrete can be characterized by the flexural-to-compressive strength ratio (FCR). After freeze-thaw cycles, the FCR of mPCM-modified concrete is illustrated in Fig. 4. It is evident that mPCM incorporation enhances the toughness of concrete. Compared to the P0 group, the FCR of the P3 and P6 groups (containing 3% and 6% mPCM, respectively) increases by 4.37% and 13.68%, indicating an improvement in concrete toughness. However, as the mPCM content further increases, particularly at 9% (P9) and 12% (P12), the FCR declines. Specifically, the FCR of the P9 group decreases by 9.65% compared to P6, while the P12 group experiences a 13.11% reduction relative to P6.

This phenomenon suggests that excessive mPCM may inhibit the complete hydration of cement, leading to an insufficiently developed cementitious matrix. The bridging and crack-arresting effects of mPCM significantly mitigate crack propagation, resulting in a smaller reduction in flexural strength than in compressive strength. Consequently, the incorporation of mPCM enhances the overall toughness of concrete.

Variation in splitting tensile strength

According to the data presented in Fig. 5, after undergoing freeze-thaw cycles, the splitting tensile strength of the P3 and P6 groups increased by 16.47% and 30.72%, respectively, compared to the P0 group. This indicates that the incorporation of mPCM can enhance the splitting tensile strength of concrete. However, the splitting tensile strength of the P9 and P12 groups decreased by 32.64% and 36.75%, respectively, compared to the P6 group. As the mPCM content increased, the damage to the concrete became more severe after freeze-thaw cycles, leading to a significant reduction in tensile strength. Nevertheless, this trend still demonstrates that an appropriate amount of mPCM, particularly at a 6% dosage, can significantly improve the splitting tensile strength of concrete subjected to freeze-thaw cycles. The microencapsulated structure of mPCM plays a crucial role in regulating

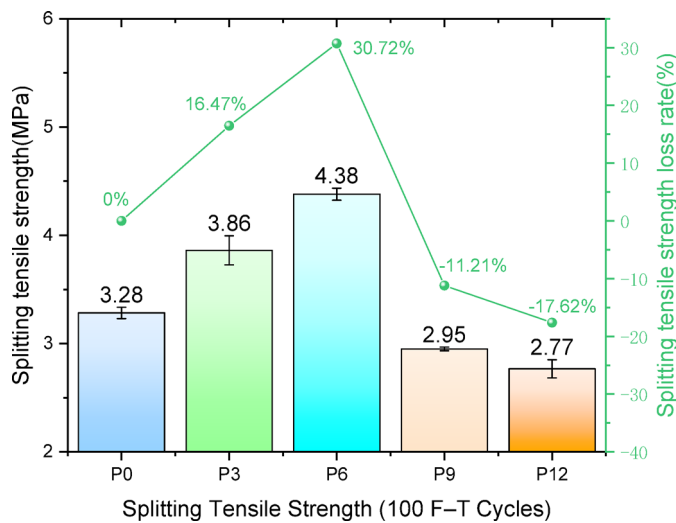


Fig. 5. Splitting tensile strength of mPCM-modified concrete.

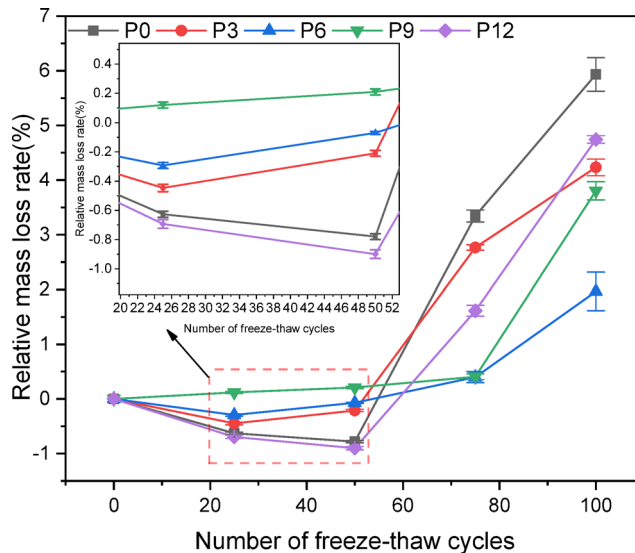


Fig. 6. Mass Loss Rate of mPCM-Modified Concrete.

temperature-induced stress and mitigating crack propagation caused by temperature fluctuations during freeze-thaw cycles, thereby enhancing the tensile strength of concrete. However, excessive mPCM content (e.g., in the P9 and P12 groups) can lead to a decline in mechanical performance, primarily due to weakened interfacial bonding, which adversely affects the overall structural integrity of the concrete. Based on the experimental results, a 6% mPCM dosage is the optimal choice, as it effectively enhances the freeze-thaw resistance of concrete while maintaining favorable mechanical properties.

Effect of Freeze-Thaw cycles on the Frost resistance of concrete

Mass loss rate

In this study, concrete specimens with different mPCM dosages underwent carbonation treatment for 14 and 28 days before being subjected to freeze-thaw damage tests. The relative mass loss of each specimen group was measured. In Eq. 1, the mass loss rate ΔM_n is defined as the ratio of the mass loss after n freeze-thaw cycles to the initial mass, where M_0 represents the mass before freeze-thaw cycles, and M_n represents the mass after n freeze-thaw cycles.

As shown in Fig. 6, the values of ΔM_n for all mPCM-modified concrete groups were lower than that of the P0 group. The mass loss rates ΔM_{100} for P0 and P3 were 6.1% and 4.5%, respectively. This indicates that incorporating mPCM significantly enhances the spalling resistance of concrete under freeze-thaw cycles. Furthermore, as the mPCM dosage increased, the mass loss rate ΔM_n initially decreased and then increased. When the mPCM content was 6%, the mass loss rate reached its minimum, with a ΔM_{100} value of 1.6%,

demonstrating the strongest freeze-thaw spalling resistance. However, when the mPCM content increased to 9% and 12%, the mass loss rate ΔM_n increased compared to P6 but remained lower than that of P0. This suggests that the addition of mPCM can further improve the freeze-thaw spalling resistance of cementitious materials.

The improvement in freeze-thaw resistance can be attributed to the randomly distributed mPCM particles, which enhance the overall integrity of concrete and mitigate surface spalling during freeze-thaw cycles. In conclusion, the incorporation of mPCM significantly improves the durability and stability of concrete under freeze-thaw cycles, reducing mass loss. Moreover, an appropriate dosage of mPCM not only enhances frost resistance but also improves the internal structure of concrete, minimizing microcrack propagation and increasing overall durability.

$$\Delta M_n = \frac{M_0 - M_n}{M_0} \times 100\% \quad (1)$$

Relative dynamic elastic Modulus

The relative dynamic elastic modulus P_n of mPCM-modified concrete is calculated using Eq. (2), where f_0 and f_n represent the transverse fundamental frequencies of the specimen before freeze-thaw cycles and after n freeze-thaw cycles, respectively.

$$P_n = \frac{f_n^2}{f_0^2} \times 100\% \quad (2)$$

As shown in Fig. 7, the loss rate of the relative dynamic elastic modulus increases with the number of freeze-thaw cycles, and different mPCM dosages influence this loss rate. Overall, the incorporation of mPCM reduces the degradation of dynamic elastic modulus during freeze-thaw cycles, with the P6 group exhibiting the lowest loss rate, indicating that an appropriate mPCM dosage (6%) effectively enhances concrete's frost resistance. However, when the mPCM content further increases to 9% (P9) and 12% (P12), the loss rate of dynamic elastic modulus rises again, suggesting that excessive mPCM incorporation may weaken the freeze-thaw resistance of concrete.

This phenomenon can be attributed to the phase-change energy storage properties of mPCM and its impact on the microstructure of concrete. During freeze-thaw cycles, temperature fluctuations induce thermal stress within concrete, particularly in stress-concentrated areas such as the interfacial transition zone (ITZ) and regions where air voids accumulate, making crack propagation more likely. Excessive mPCM dosage may lead to poor dispersion within the concrete matrix. As the mPCM content increases, microcapsules may aggregate, forming larger voids or microcracks, which not only diminish the thermal regulation function of mPCM but also compromise the strength and toughness of the concrete matrix, thereby increasing the risk of crack propagation during freeze-thaw cycles.

Additionally, the phase-change energy storage effect of mPCM is dosage-dependent. Beyond a certain threshold, the phase-change capacity of microcapsules may become saturated or ineffective, failing to alleviate thermal stress variations within concrete. Under such conditions, the heat storage and release functions of mPCM are significantly weakened, rendering it ineffective in mitigating the adverse effects of temperature gradients on concrete and potentially impairing its freeze-thaw resistance.

Therefore, although mPCM significantly enhances the frost resistance of concrete, excessive dosage negatively affects the concrete microstructure, leading to a decline in freeze-thaw resistance. Conversely, an optimal mPCM dosage ensures that the microcapsule structure absorbs and releases heat at low temperatures, buffering temperature gradients and reducing thermal stress-induced damage to the concrete. Moreover, the microporous

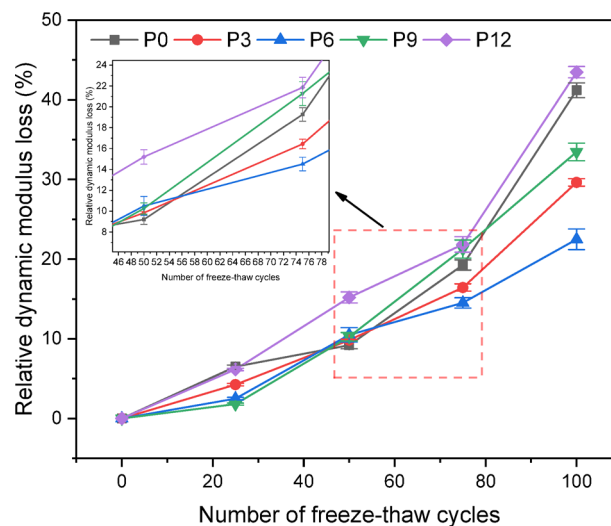


Fig. 7. Relative Dynamic Elastic Modulus of mPCM-Modified Concrete.

structure of mPCM may improve the toughness of the concrete matrix, enhancing its crack resistance during freeze-thaw cycles.

Strength loss rate of mPCM-Modified concrete

The strength loss rates of compressive strength, flexural strength, and splitting tensile strength, denoted as $\Delta f_{c,100}$, $\Delta f_{f,100}$, $\Delta f_{s,100}$, respectively, were calculated according to Eq. (3). In this equation, $f_{c,0}$, $f_{f,0}$, $f_{s,0}$ represent the compressive strength, flexural strength, and splitting tensile strength of the specimens before the freeze-thaw cycles, while $f_{c,100}$, $f_{f,100}$, $f_{s,100}$ correspond to their values after 100 freeze-thaw cycles.

$$\begin{aligned}\Delta f_{c,100} &= \frac{f_{c,0} - f_{c,100}}{f_{c,0}} \times 100\% \\ \Delta f_{f,100} &= \frac{f_{f,0} - f_{f,100}}{f_{f,0}} \times 100\% \\ \Delta f_{s,100} &= \frac{f_{s,0} - f_{s,100}}{f_{s,0}} \times 100\%\end{aligned}\quad (3)$$

The incorporation of mPCM significantly influenced the strength loss rate of concrete during freeze-thaw cycles. As shown in Fig. 8, the control group (P0) exhibited compressive, flexural, and splitting tensile strength loss rates of 25.59%, 23.14%, and 22.09%, respectively, after 100 freeze-thaw cycles. In contrast, the P6 group (containing 6% mPCM) demonstrated a significant reduction in strength loss, with compressive strength loss decreasing to 12.25%, while the flexural and splitting tensile strength loss rates were 11.74% and 10.36%, respectively. This indicates that an appropriate amount of mPCM helps mitigate the deterioration of concrete subjected to freeze-thaw cycles.

However, as the mPCM dosage increased further, the strength loss rates of the P9 and P12 groups showed an upward trend. Specifically, in the P9 group, the compressive, flexural, and splitting tensile strength loss rates were recorded as 17.87%, 16.36%, and 14.56%, respectively. In the P12 group, these values further increased to 19.45%, 18.46%, and 18.15%. These results suggest that while mPCM incorporation enhances freeze resistance at an optimal dosage, excessive amounts may lead to increased strength degradation, particularly in terms of compressive and flexural strength.

This phenomenon can be attributed to the inhibitory effect of excessive mPCM on the hydration process of concrete. A high dosage of mPCM may delay or impede cement hydration, reducing the formation of hydration products and weakening the compactness of the internal structure, ultimately compromising mechanical performance. Therefore, selecting an appropriate mPCM dosage is crucial to balancing freeze-thaw resistance and mechanical properties, as excessive incorporation may yield adverse effects.

Microstructural changes in concrete

Evolution of pore structure

By conducting MIP tests on specimens from the P0, P3, P6, P9, and P12 groups, the influence of different mPCM dosages on concrete pore size distribution and pore structure was analyzed. According to Wu Zhongwei's classification³³, pore sizes are divided into harmless pores (0–20 nm), less harmful pores (20–50 nm), harmful pores (50–200 nm), and more harmful pores (> 200 nm). The proportion of each pore type was calculated using Eq. (4).

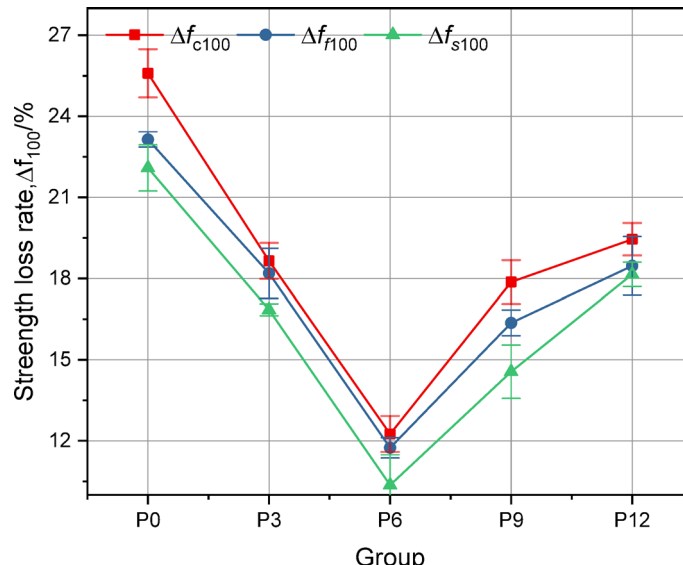


Fig. 8. mPCM-Modified Concrete Strength loss rate.

$$P_i = \frac{V_i}{V_{total}} \times 100\% \quad (4)$$

where P_i represents the proportion of pore type i (such as harmless or harmful pores), V_i denotes the pore volume within the corresponding pore size range, and V_{total} represents the total pore volume. This method allowed for the determination of the percentage distribution of pores across different pore size categories.

As shown in Fig. 9 compared with the P0 group, the P6 group exhibited significant changes in pore distribution. The log-differential intrusion curve in Fig. 9(b) shows that the number of small pores significantly decreased in P6, while the proportion of more harmful pores (> 200 nm) increased, shifting the overall pore size distribution towards larger diameters. The cumulative pore volume curve in Fig. 9(a) indicates that the peak for P0 is closer to the larger pore size region, whereas the P6 group displays a more uniform and smoother distribution. Figure 9(c) further demonstrates that with increasing mPCM content, the proportion of harmless and less harmful pores decreases, while the proportion of harmful and more harmful pores increases. Large pores can accommodate more water during freeze–thaw cycles, which may increase frost heaving risk, as larger pores tend to retain water and aggravate freeze–thaw damage. However, further analysis (see Table 3) reveals that the P6 group's average pore diameter (65.20 nm) and critical pore diameter (19.93 nm) are still lower than those of the P0 group (82.21 nm and 23.41 nm, respectively), indicating that although some larger pores appear, the overall pore structure is more refined and stable, which helps maintain structural toughness.

Meanwhile, the pore structures of the P9 and P12 groups also show distinct features. Although their average pore diameters (P9: 56.69 nm, P12: 48.19 nm) are further reduced compared to P6, which superficially suggests improved pore densification, the proportion and connectivity of harmful and more harmful pores increase, leading to higher water retention and frost heaving risk. Combined with the compressive strength results, it can

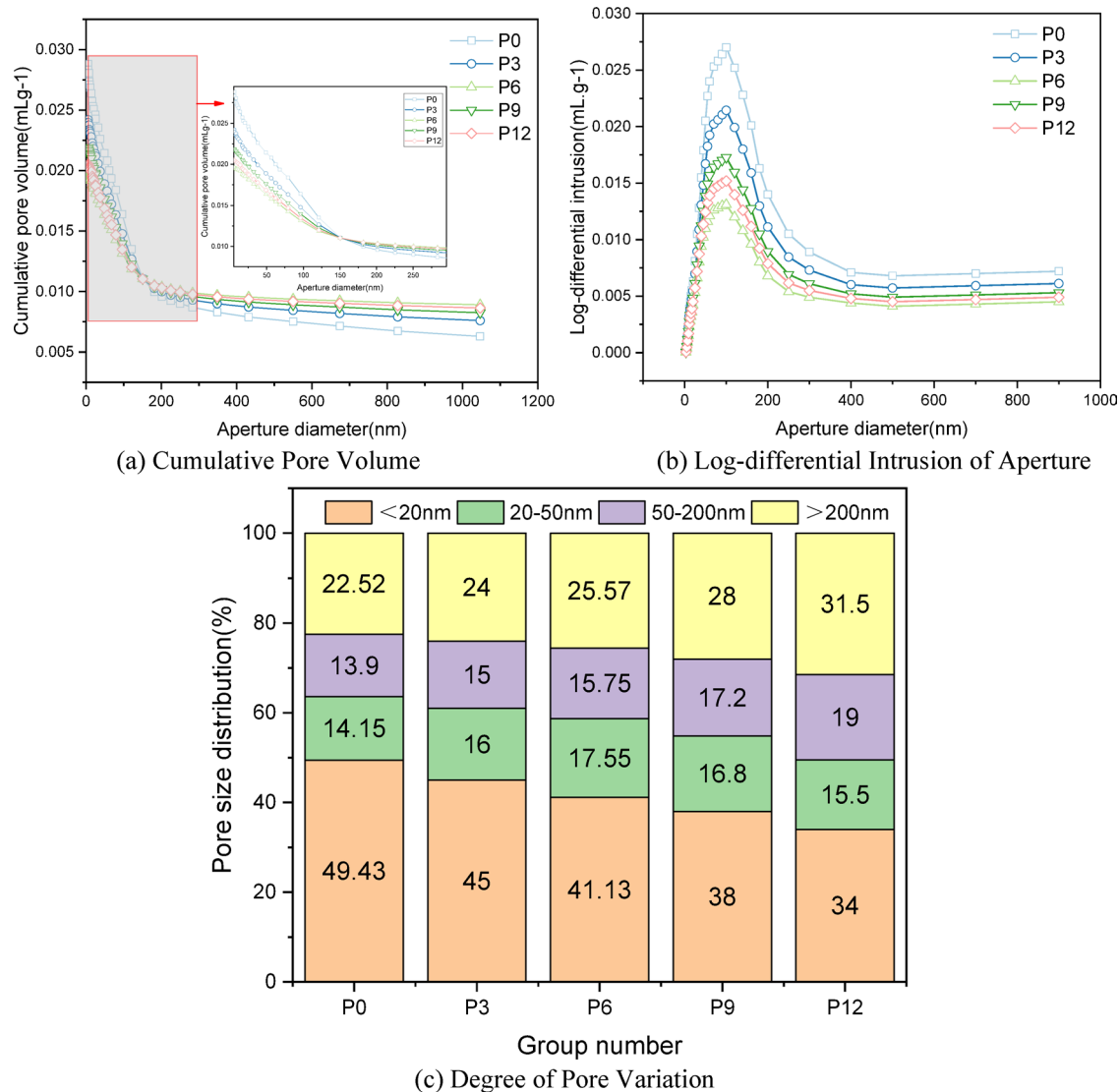
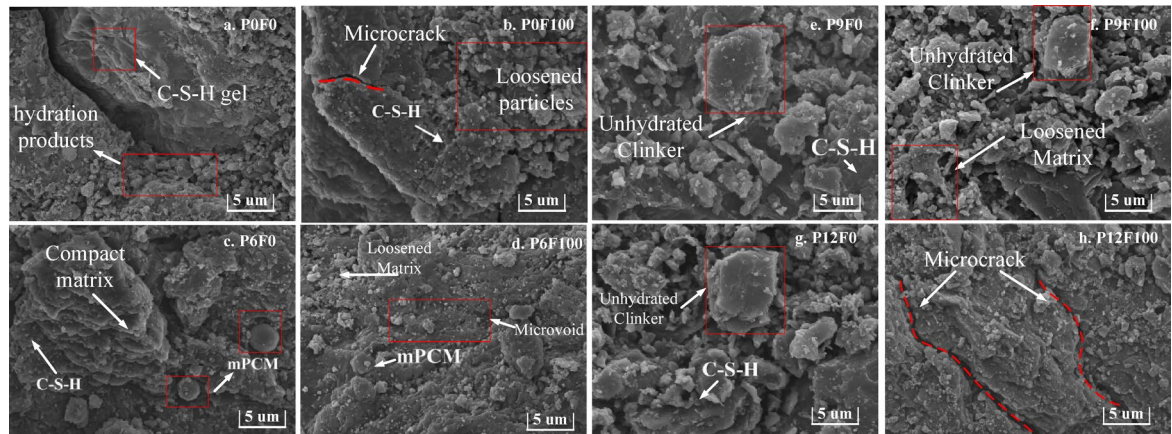


Fig. 9. Pore structure.

Group	Porosity (%)	Mean aperture (nm)	Critical aperture(nm)	Total pore area(m ² /g)	Tortuosity
P0	4.88	82.21	23.41	0.95	7.53
P3	5.82	73.70	21.67	1.32	6.43
P6	6.77	65.20	19.93	1.69	5.34
P9	7.71	56.69	18.19	2.06	4.24
P12	8.66	48.19	16.45	2.43	3.15

Table 3. Pore structure characteristics of concrete in different groups.**Fig. 10.** Microstructure of Concrete after Freeze-thaw Cycle.

be seen that although the pore diameter in P9 and P12 decreases, the higher mPCM content inhibits cement hydration, increases pore connectivity, and introduces interfacial defects, which ultimately weaken the internal load-bearing capacity. As a result, the compressive strength of P9 and P12 after 100 freeze-thaw cycles remains lower than that of the P0 group. This indicates that reduced pore size alone does not determine performance; pore connectivity and hydration degree play equally important roles. Therefore, the pore structure findings align with the mechanical performance results, highlighting that the mPCM dosage should be carefully controlled within an appropriate range.

More importantly, the phase change heat absorption mechanism of mPCM helps reduce local temperature gradients in pores during early freezing, slowing down ice crystal formation and expansion, which in turn lowers pore pressure gradients and mitigates microcrack propagation. In the P6 group, this thermal regulation effect works synergistically with the optimized pore distribution to better absorb and relieve expansion stress, thus providing structural protection during freeze-thaw cycles. Large pores may partially act as stress relief zones, while the thermal response of mPCM further suppresses abrupt freezing and ice crystal growth.

In summary, although the P6 group shows a slight increase in large pore proportion, the combination of mPCM's thermal buffering and refined pore structure enables the concrete to maintain good durability under freeze-thaw cycling, confirming the synergistic effect of dual mechanisms (thermal regulation + pore structure optimization) in enhancing frost resistance.

Microstructural morphology analysis

To further reveal the influence of mPCM incorporation on the microstructure of concrete, scanning electron microscopy (SEM) was employed to observe four groups (P0, P6, P9, and P12) before and after freeze-thaw exposure (F0 and F100), as shown in Fig. 10. The images provide clearer evidence that mPCM affects the morphology of cement hydration products, the development of microcracks, and the compactness of the matrix under different freeze-thaw states.

Before freeze-thaw cycles (F0), the P0 group exhibited a dense and continuous hydration structure, with tightly bonded C-S-H gel layers and very few visible pores or cracks. After 100 cycles (F100), obvious cracks can be seen penetrating the C-S-H region, the original gel continuity is disrupted, pore content increases significantly, and local detachment of particles occurs, indicating interfacial deterioration.

For the P6 group, the F0 condition shows uniformly distributed mPCM microcapsules embedded within a relatively dense matrix with coexisting C-S-H gels and some flake-like unhydrated particles. After freeze-thaw exposure, although local pores increase slightly, the P6 samples still retain visible mPCM particles well-integrated into the matrix, locally impeding crack propagation and helping maintain overall compactness.

In contrast, the P9 and P12 groups show more pronounced flake-like unhydrated particles and local pore development even before exposure (F0). After F100, larger and more penetrating cracks appear, the C-S-H gel

becomes more fragmented and loosely bonded, and the overall structural integrity decreases, with higher pore connectivity and surface deterioration.

In summary, a moderate amount of mPCM (such as in P6) provides a dual “filling–buffering” effect that helps resist crack expansion, while excessive addition leads to incomplete hydration and more porous structures, making freeze–thaw damage more severe. These SEM observations support the pore structure evolution analysis and emphasize the need for further dosage and process optimization to balance thermal regulation with matrix compactness.

Conclusions

This study systematically analyzed the mechanical properties, freeze–thaw resistance, and microstructural characteristics of concrete incorporating microencapsulated phase change material (mPCM). The following conclusions were drawn:

- A critical mPCM threshold (6% cement replacement) achieves synergistic mechanical–durability enhancement, delivering 8.90%, 19.23%, and 30.72% increases in compressive strength, flexural strength, and splitting tensile strength versus plain concrete. Post 100 freeze–thaw cycles, this formulation maintains structural integrity with limited deterioration (1.6% mass loss, 22.23% retained dynamic modulus, < 15% strength loss), outperforming the relevant standards and specifications. (GB T50082-2024)
- Dose-dependent performance decay occurs beyond 9% mPCM due to increased porosity and stress concentration effects, causing compressive strength reduction from 43.5 MPa (6% mPCM) to 42.23 MPa (9% mPCM) and 36.2 MPa (12% mPCM), and flexural strength reduction from 4.32 MPa to 2.93 MPa. The excessive incorporation of mPCM leads to incomplete cement hydration and the formation of larger interconnected pores, which weaken the matrix structure and reduce mechanical performance. In contrast, an optimal dosage of 6% mPCM effectively enhances freeze–thaw resistance while maintaining mechanical stability.
- Microstructural analysis reveals that 6% mPCM enhances freeze–thaw resistance by optimizing the pore structure and distribution. Specifically, the incorporation of mPCM reduces the proportion of harmless pores (0–50 nm) while increasing the fraction of harmful pores (> 50 nm), shifting the pore size distribution toward larger pores. Despite this, mPCM mitigates freeze–thaw-induced expansion forces by regulating internal temperature fluctuations, thereby improving durability. Additionally, mPCM modifies pore connectivity, reducing isolated pores while enhancing overall freeze–thaw resistance.
- As a functional building material with thermal regulation capabilities, mPCM can enhance the freeze–thaw durability and mechanical performance of concrete, aligning with the goals of green and energy-efficient construction. Its latent heat storage and release can help alleviate temperature-induced stress and mitigate freeze–thaw damage. However, this study was limited to 100 freeze–thaw cycles under controlled laboratory conditions. The long-term durability of mPCM-modified concrete under extended cycles and complex environmental exposures (e.g., chemical attack or varying humidity) remains to be fully evaluated. Although 6% mPCM was identified as the optimal dosage in this study, further investigation is needed to refine dosage design in practical applications, ensuring improved durability while minimizing potential negative effects such as pore structure coarsening and incomplete cement hydration.

Data availability

The data that support this study are available from the corresponding author upon reasonable request.

Received: 2 April 2025; Accepted: 9 July 2025

Published online: 11 August 2025

References

1. Wang, R., Zhang, Q. & Li, Y. Deterioration of concrete under the coupling effects of freeze–thaw cycles and other actions: A review. *Constr. Build. Mater.* **319**, 126045. <https://doi.org/10.1016/j.conbuildmat.2021.126045> (2022).
2. Luo, S., Bai, T., Guo, M., Wei, Y. & Ma, W. Impact of Freeze–Thaw cycles on the Long-Term performance of concrete pavement and related improvement measures: A review. *Materials* **15** (13). <https://doi.org/10.3390/ma15134568> (2022).
3. Cui, C., Zhang, S., Chapman, D. & Meng, K. Dynamic impedance of a floating pile embedded in poro-visco-elastic soils subjected to vertical harmonic loads. *Geomech. Eng.* **15**, 793–803 (2018).
4. Shields, Y., Garboczi, E., Weiss, J. & Farnam, Y. Freeze–thaw crack determination in cementitious materials using 3D X-ray computed tomography and acoustic emission. *Cem. Concr. Compos.* **89**, 120–129. <https://doi.org/10.1016/j.cemconcomp.2018.03.004> (2018).
5. Wang, X. et al. Research on internal monitoring of reinforced concrete under accelerated corrosion, using XCT and DIC technology. *Constr. Build. Mater.* **266**, 121018. <https://doi.org/10.1016/j.conbuildmat.2020.121018> (2021).
6. Junaid, M. F. et al. Inorganic phase change materials in thermal energy storage: A review on perspectives and technological advances in Building applications. *Energy Build.* **252**, 111443. <https://doi.org/10.1016/j.enbuild.2021.111443> (2021).
7. Chen, Z., Zhang, X., Ji, J. & Lv, Y. A review of the application of hydrated salt phase change materials in Building temperature control. *J. Energy Storage* **56**, 106157. <https://doi.org/10.1016/j.est.2022.106157> (2022).
8. Liu, Y., Yang, S., Li, J., Wang, F. & Hu, S. Effect of w/c ratio and antifreeze admixture on the Frost damage of sulfoaluminate cement concrete at – 20°C. *Constr. Build. Mater.* **347**, 128457. <https://doi.org/10.1016/j.conbuildmat.2022.128457> (2022).
9. Frazier, S. D. et al. Inhibiting Freeze–Thaw damage in cement paste and concrete by mimicking nature’s antifreeze. *Cell. Rep. Phys. Sci.* **1** (6), 100060. <https://doi.org/10.1016/j.xrpp.2020.100060> (2020).
10. Yang, W. et al. Damage prediction and long-term cost performance analysis of glass fiber recycled concrete under freeze–thaw cycles. *Case Stud. Constr. Mater.* **21**, e03795. <https://doi.org/10.1016/j.cscm.2024.e03795> (2024).
11. Shaukat, R., Anwar, Z., Imran, S., Noor, F. & Qamar, A. Numerical study of heat transfer characteristics of mPCM slurry during freezing. *Arab. J. Sci. Eng.* **46** (8), 7977–7988. <https://doi.org/10.1007/s13369-021-05526-6> (2021).
12. Jayalath, A. et al. Properties of cementitious mortar and concrete containing micro-encapsulated phase change materials. *Constr. Build. Mater.* **120**, 408–417. <https://doi.org/10.1016/j.conbuildmat.2016.05.116> (2016).

13. Li, W. Q., Zhang, T. Y., Li, B. B., Cui, F. Q. & Liu, L. L. Experimental investigation on combined thermal energy storage and thermoelectric system by using foam/pcm composite. *Energy. Conv. Manag.* **243**, 114429. <https://doi.org/10.1016/j.enconman.2021.114429> (2021).
14. Mao, J. F. et al. Effect of latent heat to solidification process of phase change material. *Appl. Mech. Mater.* **174-177**, 1214–1218. <https://doi.org/10.4028/www.scientific.net/AMM.174-177.1214> (2012).
15. Wei, J., Zhang, H., Zhang, W., Liu, X. & Yang, Y. Enhancing thermal performance of energy storage concrete through MPCM integration: an experimental study. *J. Building Eng.* **91**, 109533. <https://doi.org/10.1016/j.jobc.2024.109533> (2024).
16. Hu, T. et al. Study on the Preparation and properties of TiO₂@n-octadecane phase change microcapsules for regulating Building temperature. *Appl. Therm. Eng.* **249**, 123429. <https://doi.org/10.1016/j.applthermaleng.2024.123429> (2024).
17. Marani, A., Zhang, L. & Nehdi, M. L. Design of concrete incorporating microencapsulated phase change materials for clean energy: A ternary machine learning approach based on generative adversarial networks. *Eng. Appl. Artif. Intell.* **118**, 105652. <https://doi.org/10.1016/j.engappai.2022.105652> (2023).
18. Alsaadawi, M. M., Amin, M. & Tahwia, A. M. Thermal, mechanical and microstructural properties of sustainable concrete incorporating phase change materials. *Constr. Build. Mater.* **356**, 129300. <https://doi.org/10.1016/j.conbuildmat.2022.129300> (2022).
19. Savija, B., Zhang, H. & Schlangen, E. Influence of microencapsulated phase change material (PCM) addition on (Micro) mechanical properties of cement paste. *Materials* **10** (8), 863. <https://doi.org/10.3390/ma10080863> (2017).
20. Cao, V. D. et al. Thermal analysis of geopolymers concrete walls containing microencapsulated phase change materials for Building applications. *Sol. Energy* **178**, 295–307. <https://doi.org/10.1016/j.solener.2018.12.039> (2019).
21. Pilehvar, S. et al. Physical and mechanical properties of fly Ash and slag geopolymers concrete containing different types of micro-encapsulated phase change materials. *Constr. Build. Mater.* **173**, 28–39. <https://doi.org/10.1016/j.conbuildmat.2018.04.016> (2018).
22. Djamai, Z. I., Salvatore, F., Si Larbi, A., Cai, G., Mankibi, E. & M Multiphysics analysis of effects of encapsulated phase change materials (PCMs) in cement mortars. *Cem. Concr. Res.* **119**, 51–63. <https://doi.org/10.1016/j.cemconres.2019.02.002> (2019).
23. Li, Z. X. et al. Heat transfer reduction in buildings by embedding phase change material in multi-layer walls: effects of repositioning, thermophysical properties and thickness of PCM. *Energy. Conv. Manag.* **195**, 43–56. <https://doi.org/10.1016/j.enconman.2019.04.075> (2019).
24. Sukontasukkul, P. et al. Thermal properties of lightweight concrete incorporating high contents of phase change materials. *Constr. Build. Mater.* **207**, 431–439. <https://doi.org/10.1016/j.conbuildmat.2019.02.152> (2019).
25. Yeon, J. H. & Kim, K. K. Potential applications of phase change materials to mitigate freeze-thaw deteriorations in concrete pavement. *Construction Building Materials* **177**, 202–209. <https://doi.org/10.1016/j.conbuildmat.2018.05.113> (2018).
26. Fan, X. et al. The mechanical properties and resistance against the coupled deterioration of sulfate attack and freeze-thaw cycles of tailing recycled aggregate concrete. *Construction Building Materials* **269**, 121273. <https://doi.org/10.1016/j.conbuildmat.2020.121273> (2020).
27. Marani, A. & Nehdi, M. L. Integrating phase change materials in construction materials: critical review. *Construction Building Materials* **217**, 36–49. <https://doi.org/10.1016/j.conbuildmat.2019.05.064> (2019).
28. Pilehvar, S. et al. Effect of freeze-thaw cycles on the mechanical behavior of geopolymers concrete and Portland cement concrete containing micro-encapsulated phase change materials. *Construction Building Materials* **200**, 94–103. <https://doi.org/10.1016/j.conbuildmat.2018.12.057> (2019).
29. Wei, Y., Kong, W. & Wang, Y. Strengthening mechanism of fracture properties by nano materials for cementitious materials subject to early-age Frost attack. *Cement Concr. Compos.* **119**, 104025 (2021).
30. Gencel, O. et al. Biocomposite foams consisting of microencapsulated phase change materials for enhanced Climatic regulation with reduced carbon dioxide emissions in buildings. *Constr. Build. Mater.* **448**, 138214. <https://doi.org/10.1016/j.conbuildmat.2024.4.138214> (2024).
31. Yuan, X., Wang, B., Chen, P. & Luo, T. Study on the Frost resistance of concrete modified with steel balls containing phase change material (PCM). *Materials* **14**, 4497. <https://doi.org/10.3390/ma14164497> (2021).
32. Mahedi, M., Cetin, B. & Cetin, K. S. Freeze-thaw performance of phase change material (PCM) incorporated pavement subgrade soil. *Constr. Build. Mater.* **202**, 449–464. <https://doi.org/10.1016/j.conbuildmat.2018.12.210> (2019).
33. Wu, Z. & Xu, Z. *Micromechanics of Concrete Materials and Structural Properties* (Science, 2000). (in Chinese).

Acknowledgements

The authors express their gratitude to those who provided the equipment and technical support for the testing described in this paper.

Author contributions

Z.Z. and W.S. conceived and designed the study. S.L., C.L., and P.Y. conducted the experiments and collected the data. M.G. and J.H. performed the data analysis. W.S. and Z.Z. wrote the main manuscript text. S.L. and C.L. prepared Figs. 1, 2 and 3. All authors reviewed and approved the final manuscript.

Funding

This work was supported by the China Construction Enterprise Management Association Science and Technology Research and Development Project [Grant Numbers: 2024-C-114]. The authors would like to express their gratitude for the support.

Declarations

Competing interests

The authors declare no competing interests.

Additional information

Correspondence and requests for materials should be addressed to W.S.

Reprints and permissions information is available at www.nature.com/reprints.

Publisher's note Springer Nature remains neutral with regard to jurisdictional claims in published maps and institutional affiliations.

Open Access This article is licensed under a Creative Commons Attribution-NonCommercial-NoDerivatives 4.0 International License, which permits any non-commercial use, sharing, distribution and reproduction in any medium or format, as long as you give appropriate credit to the original author(s) and the source, provide a link to the Creative Commons licence, and indicate if you modified the licensed material. You do not have permission under this licence to share adapted material derived from this article or parts of it. The images or other third party material in this article are included in the article's Creative Commons licence, unless indicated otherwise in a credit line to the material. If material is not included in the article's Creative Commons licence and your intended use is not permitted by statutory regulation or exceeds the permitted use, you will need to obtain permission directly from the copyright holder. To view a copy of this licence, visit <http://creativecommons.org/licenses/by-nc-nd/4.0/>.

© The Author(s) 2025